Mausam, (1990), **41**, 1, 21-30

551.513.1 (267)

Time-mean atmospheric circulation and diabatic heating over the Arabian Sea during July

KSHUDIRAM SAHA
27, *B-Road, Maharani Bagh, New Delhi*
and
SURANJANA SAHA
Dept. of Met., Univ. of Maryland, College Park, MD 20742, *USA*

(*Received 10 March 1988*)

सार — अन्तरराष्ट्रीय हिन्द महासागर अभियान से प्राप्त चार वर्षीय (1963-66) के माध्य जुलाई मौसम विज्ञान संबंधी आंकड़ों का प्रयोग करते हुए उर्ध्वाधर गति का आकलन किया गया है, जो अरब सागर तथा आसपास के क्षेत्रों में उर्ध्वाधर परिचालन कोशिकाओं का निगमन करता है। इन आंकड़ों का प्रयोग ऊश्मा संतुलन समीकरण का प्रयोग करते हुए डायबेटिक ऊष्मन को आकलित करने के लिए आकलित उर्ध्वाधर गति के साथ भी किया गया है। परिणामों में यह पता चलता है कि डायबेटिक उष्मन अरब सागर क्षेत्र में वायुमंडलीय परिचालन के लिए मुख्य प्रेरक क्रिया-विधि बनाते हैं, यद्यपि ऊष्मा संवहन ऊष्मा बजट को, मुख्य रूप से पश्चिमी अरब सागर में, काफी योगदान देता है जिसके फलस्वरूप अनुमानित संबंध $Q/c_p \simeq -\sigma\,\omega$ को मान्यता देते हैं जहां पर Q डायबेटिक ऊष्मन की दर है, c_p नियत दाब में वायु की विशिष्ट ऊष्मा है, ω ऊर्ध्वाधर p-वेग है और σ स्थैतिक स्थायित्व प्राचल है। जहां पर प्रबल डायबेटिक शीतलन और अवतलन है वहां पर समुद्र के पूर्वी और उत्तरी भागों पर आकलित उर्ध्वाधर परिचालन कोशिका (वाकर, हैडले और मानसून) की अपनी ढलती शाखायें है और जहां मानसून द्रोणी क्षेत्र की शक्तियों से बढ़े हुए संवहन में वर्षा के कारण प्रबल डायबेटिक ऊष्मन होते हैं वहां पर समुद्र के पूर्वी भाग में उठती हुई शाखायें हैं। समुद्र के पश्चिमी भाग पर प्रबल अवतलन प्रेक्षित परिसीमा स्तर प्रक्रियायें जैसे निम्न स्तर तापमान प्रतिलोमन और सोमाली जेट को बनाये रखने में पूरा सहयोग प्रदान कर सकते हैं।

ABSTRACT. Using the four-year (1963-66) mean July meteorological data of the International Indian Ocean Expedition, the study computes vertical motion and deduces vertical circulation cells over the Arabian Sea and surrounding areas. The data are also used along with computed vertical motion to compute diabatic heating using the heat balance equation. The results suggest that diabatic heating constitutes the main forcing mechanism for atmospheric circulation in the Arabian Sea region, even though thermal advection makes an appreciable contribution to the heat budget especially over the western Arabian Sea, thereby validating the approximate relationship, $Q/c_p \simeq -\sigma\ \omega$, where Q is the rate of diabatic heating, c_p is the specific heat of air at constant pressure, ω is the vertical p-velocity and σ is the static stability parameter. The computed vertical circulation cells (Walker, Hadley and monsoon) have their sinking branches over the western and northern parts of the sea where there is strong diabatic cooling and subsidence and rising branches over the eastern part of the sea where strong diabatic heating due to precipitation in the monsoon trough zone forces enhanced convection. Strong subsidence over the western part of the sea may well help maintain the observed boundary layer processes such as low-level temperature inversion and the Somali jet.

1. Introduction

Contrary to the usual text-book model of tropical monsoons (see, *e.g.*, Holton 1979), which shows strong penetrative convection over the heated land and subsidence over the relatively cool sea, several studies (*e.g.*, Sawyer 1947, Ramage 1966, Blake *et al.* 1983, Luo and Yanai 1983) testify that convection in the 'heat low' over land to the north and west of the Arabian Sea is confined to a very shallow layer (~1 km) above the land surface, while the whole troposphere aloft is dominated by strong subsidence. The observed subsidence is primarily due to radiative heat loss in a distinctly dry continental atmosphere over the land and it is this tropospheric subsidence that restricts land convection to a shallow layer. There have been few studies of vertical motion over the sea. However, observed distributions of cloud and precipitation suggest the existence of a deep layer of convection over the eastern part of the Arabian Sea, the western part being dominated by strong subsidence and extreme dryness above a shallow layer of moist convection (~ 1 km). Ramage (1966) finds an inverse relationship between surface pressure in the heat low over northwest India and adjoining Pakistan and rainfall over the northeastern part of the Arabian Sea off Bombay. He associated the rainfall with subtropical cyclones, a case study of which was made by Miller and Keshavamurthy (1968).

We have little definitive information on the north-south (Hadley and monsoon) and east-west (Walker-type) vertical circulation cells which effect heat balance in the Arabian Sea region transferring heat from source to sink. The zonally averaged mean meridional circulation of the summer hemisphere does not reveal a Hadley cell if the averaging is done over longitudes which include the monsoon region (Schulman 1973). However, Rao (1962) who studied the mean meridional circulation over the Indian region finds that the monsoon

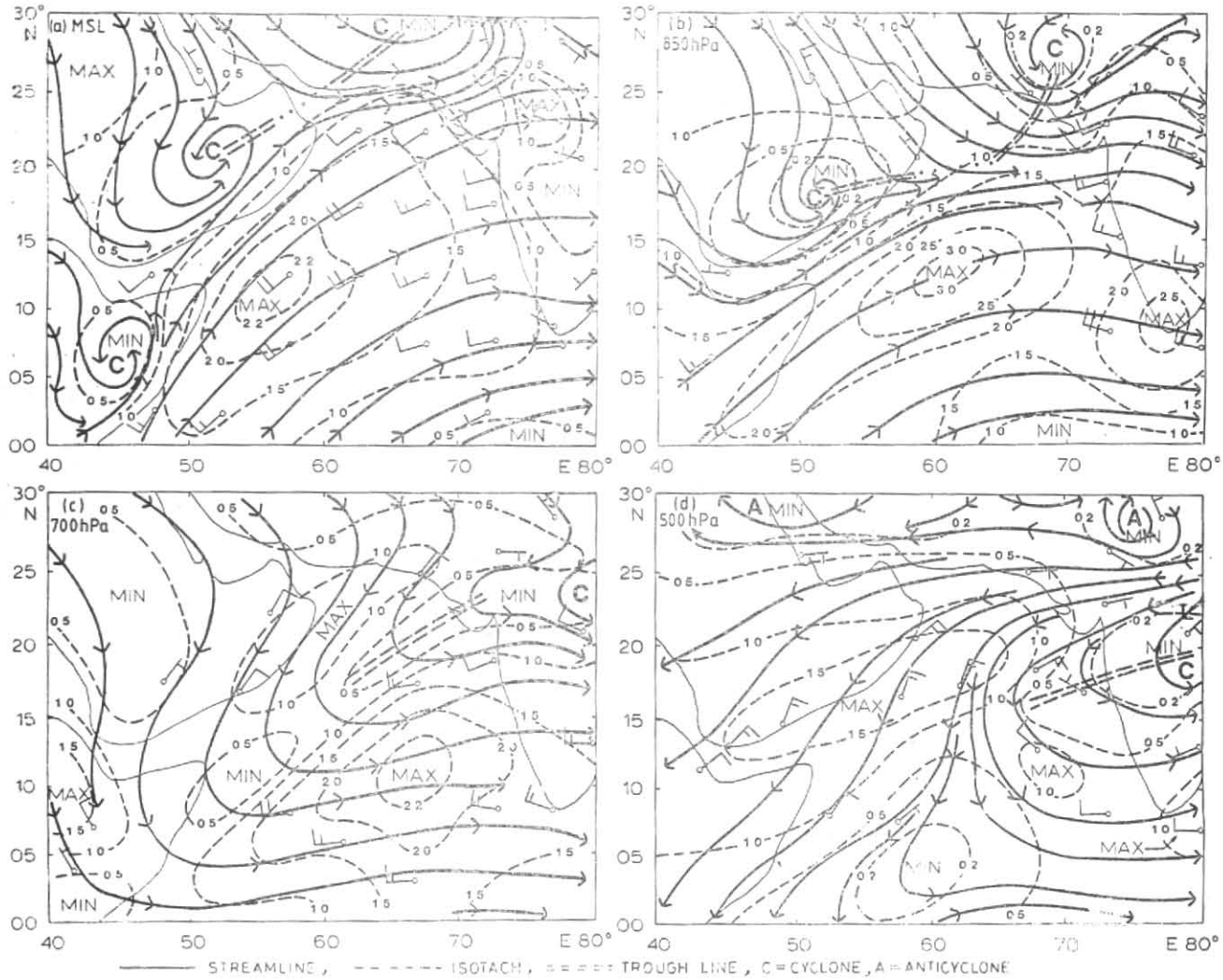

Figs. 1 (a-d). Streamline (continuous)-isotach (dashed) analysis based on plotted wind data (speed in knots) at : (a) m.s.l.; (b) 850 hPa; (c) 700 hPa and (d) 500 hPa. Double-dashed line represents the troughline. C–Cyclonic, A–Anticyclonic.

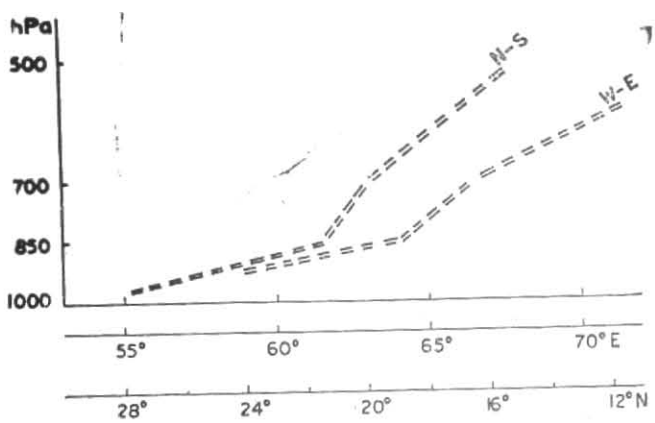

Fig. 2. Southward (N–S) and eastward (W-E) slope of the troughline with height over the Arabian Sea

cell (southerlies below, northerlies above) lies south of the Hadley cell (northerlies below, southerlies above) north of 25°N, while to the south there is no Hadley cell at all but the monsoon cell. Few studies have investigated the east-west Walker circulation and it is not known whether this type of vertical circulation exists over the Arabian Sea region at all. Some recent studies (*e.g.*, Krishnamurti and Ramanathan 1982, Pearce and Mohanty 1984) which deal with the problem of onset of the summer monsoon over the Arabian Sea highlight the importance of differential heating in the evolution of the monsoon current over the sea about the time of onset.

In the present study, we use some of the observed features of the time-mean July atmosphere over the Arabian Sea and littoral countries to compute vertical motion and vertical circulation cells with the objective of

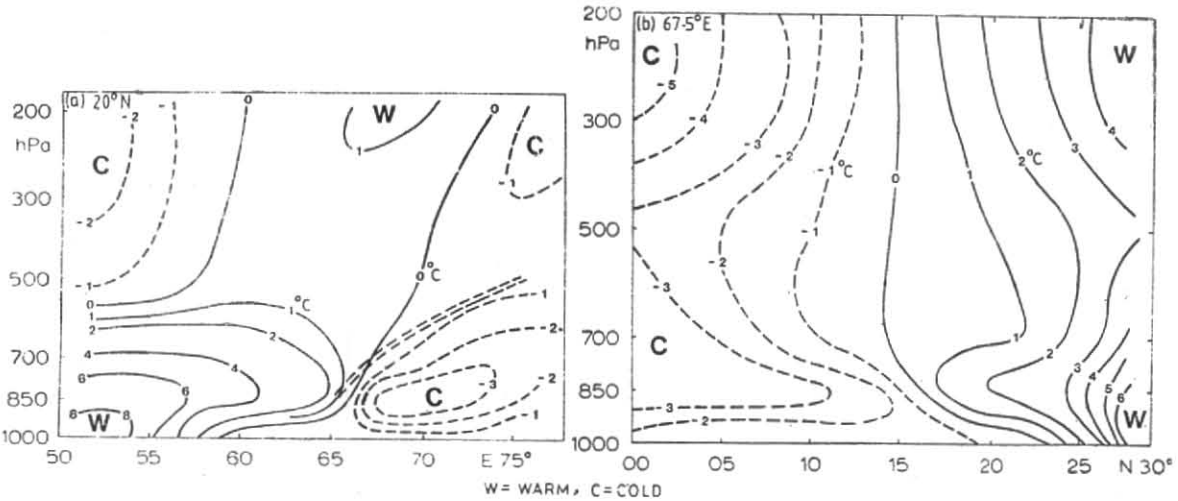

Figs. 3 (a-b). Vertical cross-sections showing the distributions of : (a) zonal temperature anomaly (°C) along 20°N and (b) Meridional temperature anomaly (°C) along 67.5°E. W–Warm, C–Cold.

checking their consistency with the distributions of diabatic heating and cooling and the requirements of heat balance over the region. The study also examines the possible influence of the vertical circulation cells on some of the observed features of the boundary layer such as convection, temperature inversion, etc.

2. Data and analysis

Data used for the study are the monthly mean data for July (1963–66) when the summer monsoon is fully established over the Arabian Sea and surrounding areas and are obtained from the sources : (*i*) *Meteorological Atlas of the International Indian Ocean Expedition (IIOE) for station data at surface* (Ramage *et al.* 1972 a), (*ii*) *Meteorological Atlas of the IIOE for station data in the upper air* (Ramage and Raman 1972b) and (*iii*) *The WMO Monthly Climatic Data of the World.* In a preface to their publication, Ramage and Raman (1972 b) give an account of the IIOE data collected by the special observing platforms, such as ships, aircraft, ocean weather buoys, etc along with the routine meteorological data, which went into the processing of the monthly mean data, which will not be repeated here. *The Monthly Climatic Data of the World* supplemented the data coverage over the littoral countries. The basic data include the geopotential height, wind (V), temperature (T) at the standard pressure surfaces 1000, 850, 700, 500, 300, 200 and 100 hPa and dew-point at m.s.l., 850, 700, 500 and 300 hPa over the area bounded by the equator and 30° N and longitudes 40°E and 80°E. Station data plotted on maps are analysed manually for fields of winds, temperature and humidity-mixing-ratio. The analysed data are placed in a 2° Lat. -2.5° Long. grid for further study and computations.

3. Time-mean meteorological fields

The 4-year mean (1963-66) July fields of wind, temperature and humidity-mixing-ratio are briefly described in the subsections that follow.

(a) *Wind field*

Figs. 1 (a-d) present the streamline-isotach analyses along with plotted data, at m.s.l. (≃1000 hPa), 850, 700 and 500 hPa respectively. Amongst other features, they reveal the following important characteristics of the mean wind field :

(*i*) A troughline (indicated by a double-dashed line) in the circulation over the northern Arabian Sea. The presence of this trough is also evident in the pressure and geopotential fields (not shown). The concept of a trough in the wind field rests on quasi-geostrophic assumption which has been found to be sufficiently valid in latitudes north of 5°N (Johnson and Morth 1960). At m.s.l. (Fig. 1a), its axis, oriented in a more or less NE-SW direction passes through the centres of the 'heat low' circulations over Pakistan and Arabia (except for an apparent slight break, indicated by dots, in its continuity over the northwest corner of the Arabian Sea). The axis slopes southeastward with height (Fig. 2), the gradient being about 1/700 below 850 hPa over the western and northern parts of the sea and about 1/150 between 850 and 700 hPa over the southeastern part. The trough normally disappears above 500 hPa.

(*ii*) A low-level wind maximum in the southwest monsoon current below 700 hPa over the western part of the Arabian Sea with a speed maximum of about 22 kt at m.s.l. and 30 kt at 850 hPa. The location of the speed maximum appears to shift eastward with height.

Maps presented in Figs. 1 (a–d) show large data gaps over parts of the sea especially at 850 hPa (Fig. 1b). Over such parts we were guided in our analysis by the results of earlier studies (*e.g.*, Bunker 1965, Findlater 1969, Van de Boogaard 1977) of Arabian Sea data. Findlater (1969) in Fig. 12 of his paper shows the approximate location of the core of the low-level southwest wind maximum (> 60 kt) at about 850 hPa extending from the coast of Somalia to India across the Arabian Sea. A low level

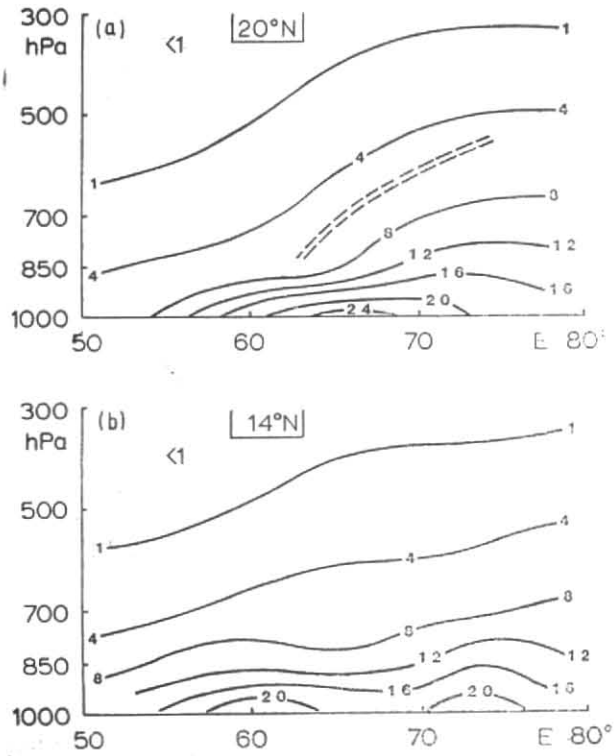

Fig. 4. Zonal-vertical distributions of humidity-mixing-ratio (g/kg) along : (a) 20°N and (b) 14°N

flight report on 1 September 1964 revealed a wind maximum of about 60 kt at a mean height of about 1.5 km a.s.l. at location 12°N, 60°E and 50 kt in the 1.0–1.5 km a.s.l. layer at 11°N, 56°E. A wind maximum of 30 kt centred at about 12°N, 60°E was used by the authors as the 4-year (1963-66) mean in the analysis (Fig. 1b).

(b) *Temperature field*

The thermal structure of the monsoon atmosphere is typified by two vertical sections shown in Figs. 3 (a & b). Fig. 3(a) shows the distribution of zonal temperature anomaly (deviation from zonal mean temperature) along 20°N and Fig. 3(b) shows the distribution of meridional temperature anomaly (deviation from meridional mean temperature) along 67.5°E. The observed meridional temperature gradient (°C/1000 km) along longitudes 60°E, 67.5°E and 72.5°E and zonal temperature gradient (°C/1000 km) along 20°N between 60°E and 70°E are presented in Table 1. Figs. 3 (a&b) and Table 1 appear to reveal the following characteristics of the thermal field :

(*i*) The northern and western parts of the Arabian Sea are decidedly warmer than the southern and eastern parts, practically throughout the troposphere :

(*ii*) Pronounced low-level temperature inversion prevails over the northern (north of about 15°N) and the western (west of about 65°E) parts of the sea, the top of the inversion layer being at about 800 hPa; and

TABLE 1

Magnitudes of the mean zonal and meridional temperature gradients (°C/1000 km) over the Arabian Sea during July

Pressure (hPa)	Zonal (60°E-70 E), 20°N	Meridional (25°N-15°N)		
		60°E	67.5°E	72.5°E
100	—1.1	0.6	3.0	2.8
200	—1.8	3.2	3.7	4.5
300	0.1	2.9	3.5	3.7
500	0.3	1.2	1.8	2.1
700	4.8	2.7	2.4	2.6
850	8.6	5.0	5.5	4.8
1000	—0.7	4.9	3.2	3.7

(*iii*) In the vertical distributions of the zonal and meridional temperature anomalies (Figs. 3 a&b), there appear to be two warm anomaly maxima, one in the lower troposphere (below about 700 hPa) and the other in the upper troposphere (above 300 hPa).

The horizontal temperature gradients presented in Table 1 and shown in Figs. 3 (a&b) appear to be strong enough to support the vertical wind shear observed over the Arabian Sea.

(c) *Humidity-mixing-ratio field*

Fig. 4 presents the vertical distribution of humidity-mixing-ratio (g/kg) in two latitudinal sections : (a) 20°N and (b) 14°N. These appear to bring out the marked contrast in the vertical distribution of moisture between the western (west of about 65°E) and the eastern parts of the sea, more so along 20°N than along 14°N. Over the western part, most of the moisture (say, >8 g/kg) is confined to a shallow layer below 850 hPa, while the troposphere above is dry or has little moisture. On the other hand, over the eastern part moisture extends through a much deeper layer up to at least 700 hPa or even beyond. A sudden jump in moisture content is clearly visible in the monsoon trough zone.

4. Vertical motion field

We compute vertical motion by integrating the continuity equation in the form :

$$\omega = \int \nabla . \mathbf{V} \, \delta p$$

where, ω is the vertical p-velocity, $\nabla . \mathbf{V}$ is the horizontal wind divergence and p is pressure.

Horizontal divergence is calculated from the wind components (u, v) using the expression :

$$\nabla . \mathbf{V} = \partial u/\partial x + \partial v/\partial y - (v/a) \tan \phi$$

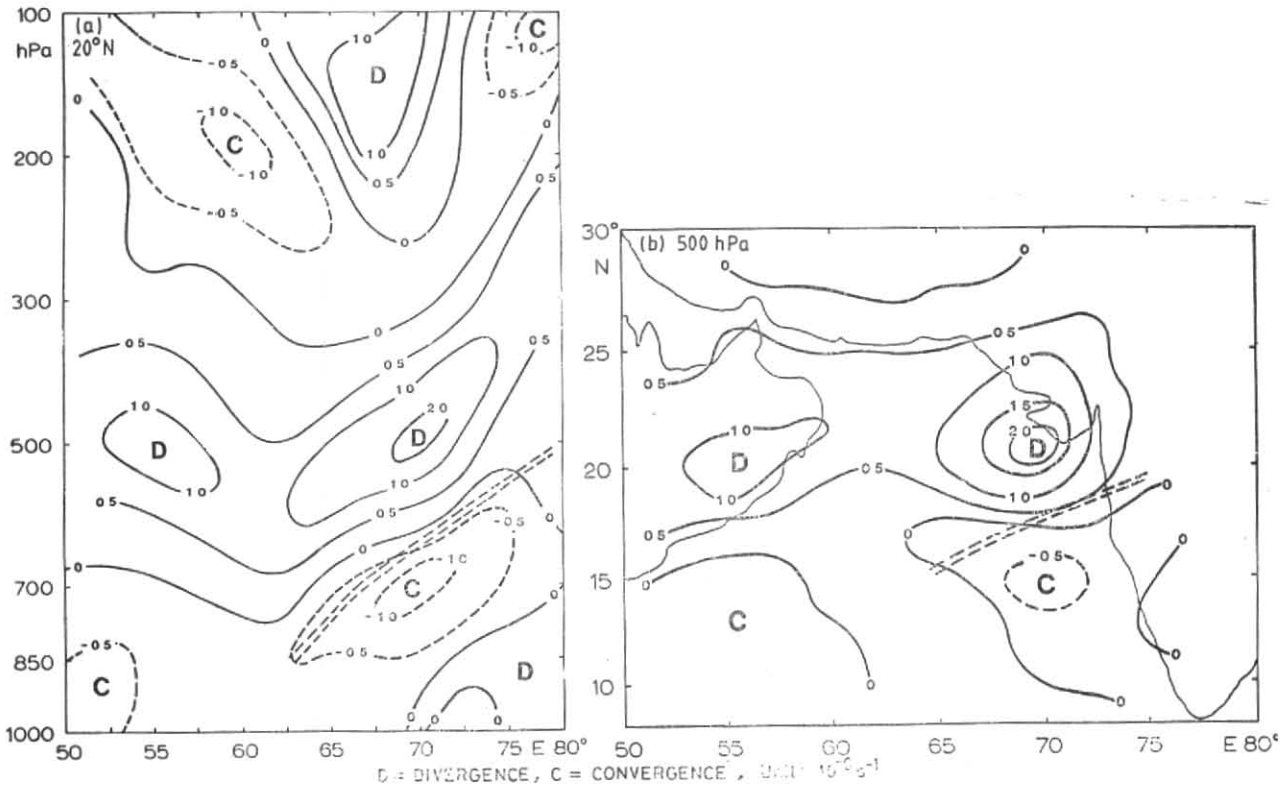

Figs. 5 (a & b). Distribution of divergence (unit : 10^{-6} s^{-1}) : (a) in a zonal-vertical cross-section along 20° N and (b) at 500 hPa. D—Divergence, C—Convergence

where, a is the mean radius of the earth and ϕ is the latitude. Space derivatives are evaluated using a centred finite-differencing scheme.

The integration is effected from the earth's surface upward, the lower boundary condition for ω being $\omega_{ps} = \mathbf{V}_s \cdot \nabla p_s$ where, p_s is the surface pressure and $\mathbf{V}_s$ is the wind at the station level (if available, otherwise the standard pressure surface immediately above the station). The well-known O'Brien's correction is applied to the computed vertical velocity at each pressure surface so as to reduce the vertical velocity at the top (~100 hPa) to zero.

Computed values of divergence and vertical motion for some selected sections are presented in Figs. 5 (a & b) and Figs. 6 (a & b) respectively. Fig. 5 (a) shows, along 20°N, divergence in the middle troposphere with convergence below and above. However, divergence appears in the upper troposphere (above 250 hPa) between about 62°E and 72°E. Fig. 5(b) which shows divergence at 500 hPa reveals strong divergence over the northern and western parts of the sea and strong convergence over the southeastern part. Fig. 6(a) shows the distribution of computed vertical motion at 500 hPa. In general, it shows strong downward motion over the northern and western parts and upward motion over the southeastern part of the Arabian Sea. Fig. 6(b) which shows the distribution of vertical velocity with height along the latitudes 26°N, 20°N and 14°N testifies that the upward motion over the southeastern part of the Arabian Sea is strongest between about 65°E and 70°E in the mid-tropospheric layer 700-500 hPa where the elevated monsoon trough has its maximum convergence. It is well-known that strong orographic lifting occurs at the lower boundary near the west coast of India during July. This, however, is not reflected in Fig. 6(a) which shows only feeble upward motion over the coastal zone, possibly because of the effect of unrealistically large low-level divergence in the upstream westerly flow (*see* Fig. 5a). According to our computations, the vertical velocity due to orography at the latitude of Bombay (~18°N) is upward (-10×10^{-4} hPa s^{-1}) on the windward side of the mountain (approximately between 72·5°E and 75°E) and downward (6.3×10^{-4} hPa s^{-1}) on the leeside (between 75°E and 77.5° E). A few pockets of feeble downward motion seen at 500 hPa over the western part of the Indian Peninsula (Fig. 6a) appears to be a part of the leeside downward motion.

5. Vertical circulation cells

A combination of the computed vertical velocity ω with the horizontal components (u,v) of the mean observed wind enables us to obtain resultant streamlines which reveal the structure of the atmospheric vertical circulation in zonal and meridional planes. Our findings in this regard are as follows.

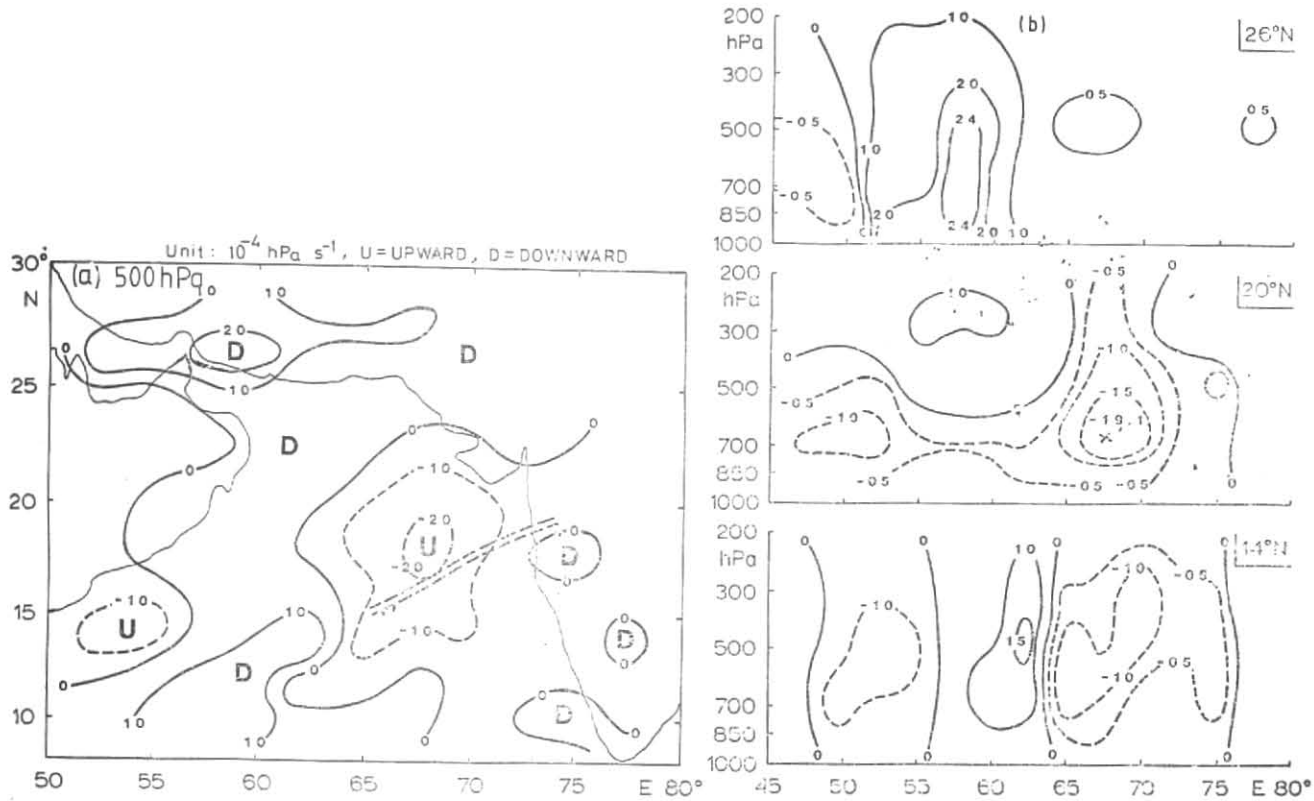

Figs. 6 (a-b). Distribution of vertical p-velocity (unit : 10^{-4} hPa s^{-1}) : (a) at 500 hPa and (b) in zonal-vertical cross-sections along 26°N, 20°N and 14°N. U-Upward, D-Downward

(a) *Zonal circulations* (u, ω)

Interesting flow features are revealed by Figs. 7(a-c) which present the resultant streamlines based on (u, ω) values along latitudes 26°N, 20°N and 14°N respectively. The section along 26°N (Fig. 7a) which lies almost wholly over land close to the northern coast of the sea has all descending motion in the low-level westerlies and upper-level easterlies. The section along 20°N (Fig. 7b) has a different story to tell. Here, the lower tropospheric westerlies rise in convection, shallow west of about 65°E but penetrative in the monsoon trough zone between 65°E and 70°E. East of 70°E convection in the westerlies appears to weaken somewhat till the current meets the Western Ghats mountains where it is lifted orographically. The resulting streamlines in the upper easterlies which have descending motion east of about 72° E also rise in strong penetrative convection over the monsoon trough zone before descending again west of about 65°E. The resultant streamlines along 14°N (Fig. 7c) show an interesting anti-clockwise vertical circulation cell centred at about 64°E between 300 hPa and 500 hPa. This cell which has strong westerlies below, upward motion to the east, easterlies above and downward motion to the west of the centre resembles a Walker (W) cell. The existence of this cell confirms a suspicion by Smith (1985) that the extensive offshore penetrative convection observed over the eastern part of the Arabian Sea (often extending 500–1000 km from the coast) is not due to the orographic blocking of the southwest monsoon current by the Western Ghats mountains as thought by many (*e.g.*, Desai 1967, Grossman and Durran 1984) but some other mechanism such as synoptic disturbances, etc. Our study reveals that penetrative convection occurs in the monsoon trough zone where the Walker cell has its rising branch and where synoptic disturbances such as offshore vortices, lows and depressions are known to form during the southwest monsoon season, though their frequency in July is extremely small. The general effect of the monsoon trough may simply be extensive cloudiness over the sea as actually observed by satellites. Any development of disturbances on the quasi-stationary mean monsoon trough will depend on dynamic instability of the flow and the growth rate of the disturbances.

(b) *Meridional circulations* (v, ω)

Resultant streamlines (v, ω) along two meridians, 60°E and 67.5°E are presented in Figs. 8 (a & b) respectively. Along 60°E (Fig. 8a) which lies over the western part of the sea, strong descending motion prevails in the whole troposphere north of about 22°N. South of this latitude, two oppositely-rotating vertical circulation cells appear

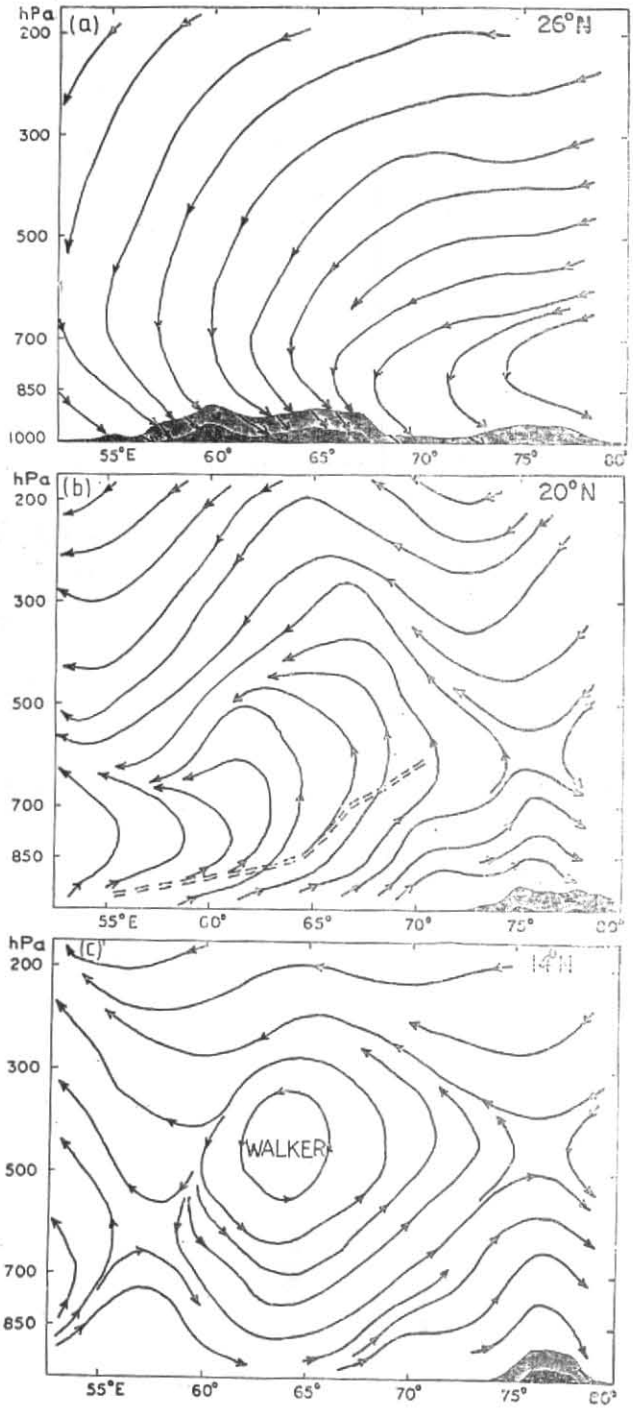

Figs. 7(a-c). Zonal-vertical cross-sections showing the resultant streamlines (u, ω) along latitudes : (a) 26°N, (b) 20°N and (c) 14° N

to be present, one a clockwise circulation cell centred at about 18°N at 250 hPa and the other an anti-clockwise circulation cell centred at about 16°N between 850 hPa and 700 hPa, both over the sea. The upper cell which has upward motion to the south & southerlies above, downward motion to the north and northerlies below the centre may be called an elevated Hadley (H) cell. The lower cell which has upward motion to the north, northerlies above, downward motion to the south and southerlies below the centre may be called a Monsoon (M) cell. Very similar feature are revealed by the meridional section along 67.5°E (Fig. 8b). However, here the elevated Hadley cell is centred over the land at about 24°N at 300 hPa, more or less in agreement with the finding by Rao (1962) while the monsoon cell is centred over the sea at about 13°N between 700 hPa and 500 hPa. The rising branches of the two cells appear to be coupled in space by the sloping monsoon trough. It is likely that a change in the strength of the elevated Hadley cell will bring about an inverse relationship between surface pressure in the 'heat low' over land and rainfall over the sea off Bombay as observed by Ramage (1966).

6. Diabatic heating and circulation

Since monsoon circulation is forced by differential heating and cooling of the different parts of the atmosphere, it is of great interest to see how far the vertical motion computed in Sec. 4 and the vertical circulation cell suggested in the foregoing section are consistent with the distributions of diabatic heating and cooling which may be computed from the heat balance equation in the form :

$$\underset{(1)}{\partial T/\partial t} = \underset{(2)}{-\mathbf{V}.\nabla T} + \underset{(3)}{\sigma\omega} + \underset{(4)}{Q/c_p}$$

where, Q is the rate of diabatic heating.

c_p is the specific heat of air at constant pressure ($=1004$ J kg^{-1} K^{-1})

t is time

$\sigma\ [= (R/c_p)T/p - \partial T/\partial p]$ is the static stability parameter and

R is the gas constant for dry air ($=287$ J kg^{-1} K^{-1}).

The basic data used in the study being time-mean (1963-66) July values, we put term (1) equal to zero and evaluate terms (2) and (3) from temperature and wind data. Term (4) is evaluated as a residual from the heat balance equation. Term (2) (thermal advection $\mathbf{V}.\nabla T$) is computed at each grid-point using a centred finite-differencing scheme. The computation takes into account the contribution of the time-mean part $\bar{\mathbf{V}}.\nabla\bar{T}$ only, leaving the eddy part $\overline{\mathbf{V}'.\nabla T'}$ which we believe to be relatively small in the monsoon region especially in the lower troposphere (here, the bar denotes time-mean and the prime deviation from time-mean). Term (3) ($\sigma\omega$) requires computation of σ besides ω which we have already computed in section 4. We compute σ at a pressure surface from the temperature and pressure values at the surface (T/p) and the temperature lapse rate $\partial T/\partial p$ between the pressure surfaces immediately above and below.

Results of our computation of the heat budget are presented in Figs. 9(a & b). Fig. 9 (a) shows typical vertical profiles of the terms (2), (3) and (4) at two points, one

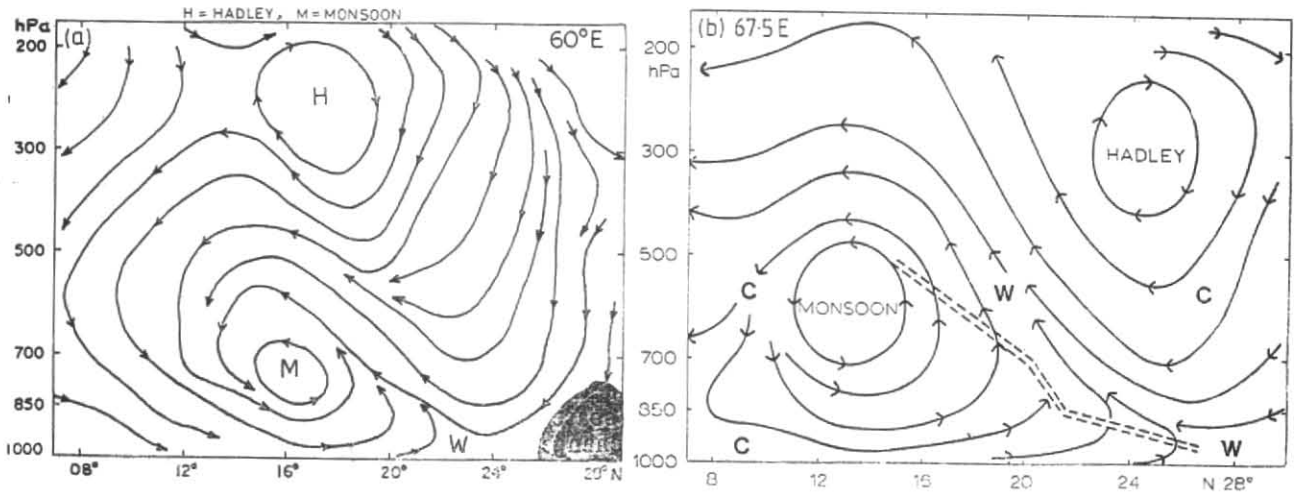

Figs. 8(a&b). Meridional-vertical cross-sections showing the resultant streamlines (v, ω) and diabatic warming (W) and cooling (C) along longitudes : (a) 60°E and (b) 67.5°E. H—Hadley, M—Monsoon

over the western Arabian Sea (14°N, 60° E) and the other over the eastern Arabian Sea (20° N, 67·5° E), the values presented at each pressure surface being average of those at the five grid-points, (i, j), $(i+1, j)$, $(i-1, j)$, $(i, j+1)$, and $(i, j-1)$, where (i, j), denotes the central point. It appears to reveal the following:

(*i*) There is warm advection ($\mathbf{V} \cdot \nabla T$ negative) in the whole troposphere above 850 hPa over the western part of the sea and in the lower troposphere below 500 hPa over the eastern part. There appears to be cold advection below 850 hPa over the western part and in a shallow layer close to the sea surface over the eastern part.

(*ii*) Diabatic heating (Q/c_p) is strongly positive (negative) over the eastern (western) part of the sea. It appears to be negative over the eastern part below 850 hPa. Strongest diabatic heating or cooling appears to occur at about 700 hPa.

(*iii*) The effect of diabatic heating (cooling) is largely compensated by adiabatic cooling (heating) due to upward (downward) motion ($\sigma\omega$). This means that approximaterly. $Q/c_p \simeq -\sigma\omega$. Fig. 9(b) presents the horizontal distribution of the vertically-integrated (between 925 hPa and 150 hPa) diabatic heating during July. It shows strong negative values (diabatic cooling) over the northern and western parts of the Arabian Sea and adjoining land areas of Arabia, Iran, Pakistan and northwest India. To offset this diabatic cooling, air must subside and warm up adiabatically and diverge heat at lower levels. There is clear evidence of this subsidence warming and divergence in our results (*see* Figs. 3, 5 and 6). By contrast, horizontal convergence and penetrative convection occur in the monsoon trough zone over the eastern part of the sea to offset the effect of strong diabatic heating due to precipitation in the trough zone.

In the actual atmosphere, diabatic heat sources and sinks exist over both land and sea, as shown, for example, in Fig. 8 (b) in relation to the meridional circulation along 67.5°E. These sources and sinks are largely generated in the atmosphere by differential response to incoming solar radiation, radiative heating and cooling, sensible heat fluxes across boundaries, precipitation and evaporation processes, etc. Over the land in summer, strong insolational heating of the lower boundary creates a diabatic heat source but its effect appears to be limited to a shallow layer above the earth's surface, since the whole troposphere above which is generally dry, undergoes rapid diabatic cooling due to strong radiative heat loss. A reverse situation appears to prevail over the Arabian Sea, the surface of which in summer is relatively cooler than the overlying atmosphere and acts as a heat sink. However, moisture convergence aloft produces through precipitation in the monsoon trough zone a diabatic heat source which is strongest at about 700 hPa as shown in Fig. 9(a). It is principally through the vertical circulation cells that heat balance is achieved between the diabatic heat source and sink.

7. Summary

The findings of the present study may be summarized as follows :

(*i*) A quasi-stationary monsoon trough associated with the 'heat low' circulation over the Arabian Sea region

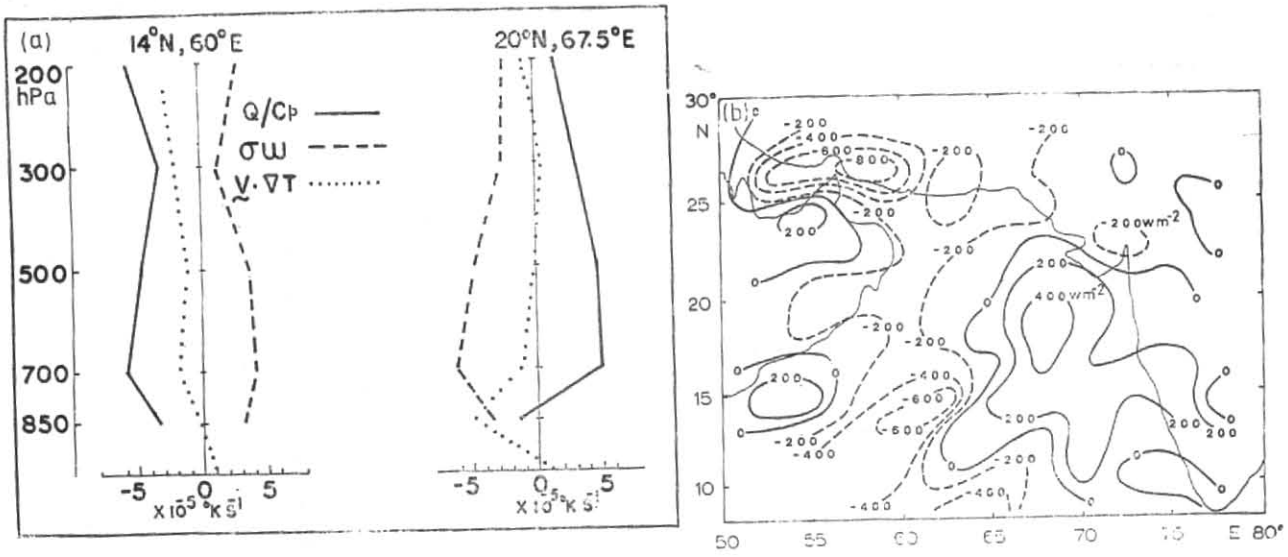

Figs. 9 (a&b). Computed values of the terms of the heat budget : (a) Vertical distributions of Q/cp, $\sigma\omega$ and $\mathbf{V}.\nabla T$ at 14° N, 60° E and 20°N, 67.5°E (unit : 10^{-5} K s^{-1}) and (b) horizontal distribution of the vertically-integrated diabatic heating Q (unit : W m^{-2}) over the Arabian Sea and surrounding areas

shifts southeastward with height to be located over the eastern part of the sea (east of about 65°E) between 850 hPa and 500 hPa. It marks the boundary between the land and the oceanic circulations.

(*ii*) The atmosphere over the land has a diabatic heat source at the lower boundary and a diabatic heat sink in the middle and upper troposphere with the result that land convection is confined to a shallow layer near the ground while strong subsidence occurs aloft. The atmosphere over the sea, on the other hand, has a diabatic heat sink both at the sea surface and aloft except in the monsoon trough zone over the eastern part of the sea where an elevated heat source exists and penetrative convection occurs. Warm subsidence over cool sea over the western part of the sea produces a pronounced low-level temperature inversion and stable stratification. It may well help maintain the low-level Somali jet.

(*iii*) Mean meridional circulation over the eastern part of the Arabian Sea consists of two vertical circulation cells, *i.e.*, a monsoon cell to the south and an elevated Hadley cell to the north, with the sloping monsoon trough forming the boundary between the two. Over the western part of the sea, the Hadley cell appears to be located almost directly above the monsoon cell with no clear-cut boundary between the two.

(*iv*) A Walker-type east-west vertical circulation cell appears to be centred at about 14°N, 64°E at 500 hPa with its sinking branch in the west and rising branch in the monsoon trough zone in the east.

(*v*) Heat budget computation suggests that despite appreciable thermal advection, dominant forcing for atmospheric circulation is diabatic heating and cooling. Thus, the relationship, $Q/c_p \simeq -\sigma\omega$, holds approximately in the Arabian Sea region.

Acknowledgments

The authors thank the Director General of Meteorology, India Meteorological Department, New Delhi, for providing facilities for this research and are grateful to Arun Attri, Jawaharlal Nehru University, New Delhi, who helped with the data processing on his personal computer (ATARI 1040 ST) and to Huug van den Dool , University of Maryland, USA who reviewed the first draft of the paper and offered useful comments. They are also grateful to the anonymous reviewer for his useful comments on this paper.

References

Blake, D.W., Krishnamurti, T.N., Low-Nam, S.V. and Fein, J.S., 1983, Heat Low over the Saudi Arabian desert during May 1979 (Summer MONEX), *Mon. Weath. Rev.*, **111**, 1759-1775.

Bunker, A.F., 1965, Interaction of the summer monsoon air with the Arabian Sea, *Proc. Symp. Met. Results of the International Indian Ocean Expedition*, Bombay, India.

Desai, B.N., 1967, The Summer Atmospheric Circulation over the Arabian Sea, *J. atmos. Sci.*, **24**, 216-220.

Findlater, J., 1969, A major low-level air current near the Indian Ocean during the northern summer, *Quart. J. R. met. Soc.*, **95**, 362-380.

Grossman, R.L. and Durran, D.R., 1984, Interactions of low-level flow with the Western Ghats mountains and off-shore convection in the summer monsoon, *Mon. Weath. Rev.*, **112**, 652-672.

Holton, J.R., 1979, *An Introduction to Dynamic Meteorology*, 2nd edition, Academic Press, New York, 391 pp.

Johnson, D.H. and Morth, H.T., 1960, Forecasting Research in East Africa, *Proc. Symp. on Tropical Meteorology in Africa* (Ed : D.J. Bargman), Munitalp Foundation, Nairobi.

Krishnamurti, T.N. and Ramanathan, Y., 1982, Sensitivity of the Monsoon Onset to Differential Heating, *J. atmos. Sci.*, **39**, 1290-1306.

Luo, H. and Yanai, M., 1983, The Large-Scale Circulation and Heat Sources over the Tibetan Plateau and Surrounding Areas during the Early Summer of 1979, *Mon. Weath. Rev.*, **111**, 922-944.

Miller, F.R. and Keshavamurthy, R.N., 1968, *Structure of an Arabian Sea Summer Monsoon System*. East-West Center Press, University of Hawaii, 94 pp.

Pearce, R.P. and Mohanty, U.C., 1984, Onsets of the Asian Summer Monsoon 1979-82, *J. atmos. Sci.*, **41**, 1620-1639.

Ramage, C.S., 1966, The Summer Atmospheric Circulation over the Arabian Sea, *J. atmos. Sci.*, **23**, 144-150.

Ramage, C.S., Miller, F.R. and Jefferies, C., 1972(a), *Meteorological Atlas of the International Indian Ocean Expedition*, **1**: *The Surface Climate*, National Science Founation, Washington D.C. 20402, pp, i-xiii + charts 1-144.

Ramage, C.S. and Raman, C.R.V., 1972(b), *Meteorological Atlas of the International Indian Ocean Expedition*, **2**: *Upper Air*, National Science Foundation, Washington D.C. 20402. pp. i-xiii + charts 1-121.

Rao, Y.P., 1962, Meridional circulations associated with the monsoons of India, *Indian J. Met. Geophys.*, **13**, pp. 157-166.

Sawyer, J.S., 1947, The Structure of the Intertropical Front over Northwest India during the SW Monsoon, *Quart. J.R. met. Soc.*, **73**, 346-369.

Schulman, L. L., 1973, On the Summer Hemisphere Hadley cell *Quart. J.R. met. Soc.*, **99**, 197-201.

Smith, R.B., 1985, Comments on 'Interactions of low-level flow with the Western Ghats mountains and off-shore convection in the summer monsoon', *Mon. Weath. Rev.*, **113**, 2176-2177.

Van de Boogaard, H., 1977, The mean circulation of the Tropical and Subtropical atmosphere—July. NCAR, Boulder, Colorado Tech. Note, NCAR/TN-118-STR, 48 pp.